

Hybrid Precoding in Millimeter-Wave Massive MIMO Systems

Ph.D. Comprehensive Examination

Pranav Jha

Student ID: 40081750

Supervisor: Dr. Wei-Ping Zhu



Department of Electrical and Computer Engineering

March 12, 2023

Outline

Technical Background

Problem Statement

Problem and Methodology I

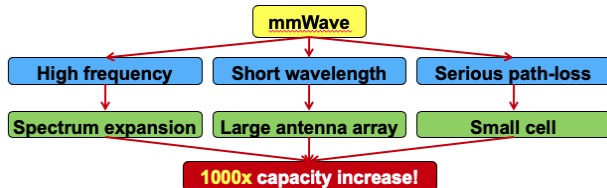
Problem and Methodology II

Critical Review

References

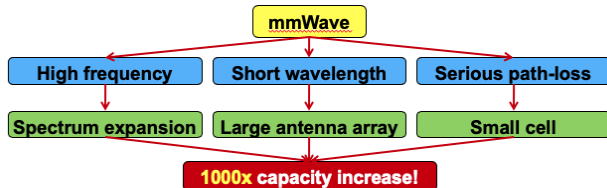
Mm-Wave Massive MIMO

Advantages



Mm-Wave Massive MIMO

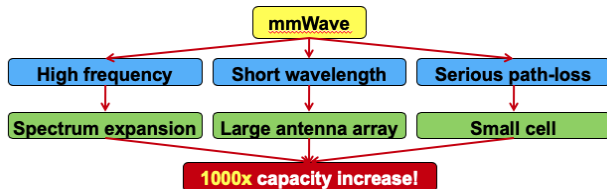
Advantages



- High frequency (30-300 GHz)
 - Larger bandwidth: 20 MHz \rightarrow 2 GHz

Mm-Wave Massive MIMO

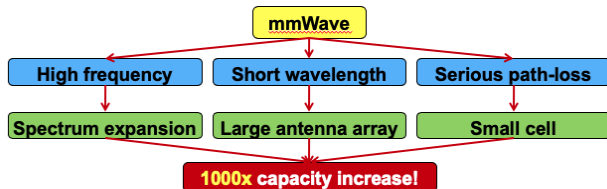
Advantages



- **High** frequency (30-300 GHz)
 - **Larger** bandwidth: 20 MHz → 2 GHz
- **Short** wavelength (1-10 mm)
 - **Enable large antenna array** (massive MIMO): At 70 GHz
 - Maximum #Antennas - 1024 and 64 (BSs and UEs)
 - Maximum #RF chains - 32 and 8 (BSs and UEs)

Mm-Wave Massive MIMO

Advantages



- **High** frequency (30-300 GHz)
 - **Larger** bandwidth: 20 MHz → 2 GHz
- **Short** wavelength (1-10 mm)
 - **Enable large antenna array** (massive MIMO): At 70 GHz
 - Maximum #Antennas - 1024 and 64 (BSs and UEs)
 - Maximum #RF chains - 32 and 8 (BSs and UEs)
- Serious **path-loss** and **blockage**
 - Massive MIMO provides sufficient gains to **compensate** the serious path-loss by using **precoding**
 - Avoid multi-cell **interference**, more appropriate for **small cell**

Precoding for Mm-Wave Massive MIMO

Traditional Precoding

- Performed in **digital domain** with optimized performance
- **One RF chain** is required to support **one** transmit antenna
- **Impractical** in energy consumption for mm-Wave massive MIMO systems
 - **250 mW** per RF chain, and **16 W** for 64 antennas¹

¹P. V. Amadori and C. Masouros, "Low RF-Complexity Millimeter-Wave BeamSpace-MIMO Systems by Beam Selection," in IEEE Transactions on Communications, vol. 63, no. 6, pp. 2212-2223, June 2015 [1]

Precoding for Mm-Wave Massive MIMO

Traditional Precoding

- Performed in **digital domain** with optimized performance
- **One RF chain** is required to support **one** transmit antenna
- **Impractical** in energy consumption for mm-Wave massive MIMO systems
 - **250 mW** per RF chain, and **16 W** for 64 antennas¹

Hybrid Analog and Digital Precoding

- Actual degree of freedom (i.e., number of users) is much **smaller** than number of antennas
- Divide digital precoding **with** large size into:
 - **Digital precoding** with **small** size
 - **Analog precoding** with **large** size (realized by phase shifter, PS)
- Significantly reduced number of RF chains
- **Power-efficient**, low complexity, without obvious performance loss

¹P. V. Amadori and C. Masouros, "Low RF-Complexity Millimeter-Wave BeamSpace-MIMO Systems by Beam Selection," in IEEE Transactions on Communications, vol. 63, no. 6, pp. 2212-2223, June 2015 [1]

Hybrid Precoding Architectures

Fully-connected Architecture

- RF chain is fully connected to all antennas
 - Large number of PSs (N^2M)
 - Near-optimal but **energy-intensive**
- Spatially sparse precoding [2]
- Codebook-based hybrid precoding [3]

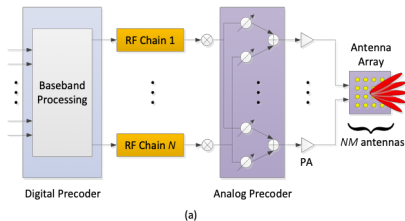
²O. E. Ayach, S. Rajagopal, S. Abu-Surra, Z. Pi and R. W. Heath, "Spatially Sparse Precoding in Millimeter Wave MIMO Systems," in IEEE Transactions on Wireless Communications, vol. 13, no. 3, pp. 1499-1513, March 2014

³W. Roh et al., "Millimeter-wave beamforming as an enabling technology for 5G cellular communications: theoretical feasibility and prototype results," in IEEE Communications Magazine, vol. 52, no. 2, pp. 106-113, February 2014

Hybrid Precoding Architectures

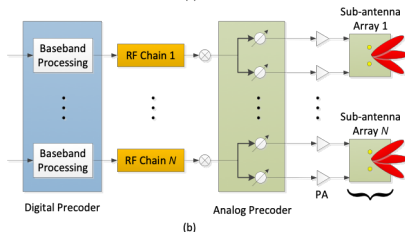
Fully-connected Architecture

- RF chain is fully connected to all antennas
 - Large number of PSs (N^2M)
 - Near-optimal but **energy-intensive**
- Spatially sparse precoding [2]
- Codebook-based hybrid precoding [3]



Sub-connected Architecture

- RF chain is partially connected to a subset of antennas
 - Smaller number of PSs (NM)
 - More **energy-efficient**



2 3

²O. E. Ayach, S. Rajagopal, S. Abu-Surra, Z. Pi and R. W. Heath, "Spatially Sparse Precoding in Millimeter Wave MIMO Systems," in IEEE Transactions on Wireless Communications, vol. 13, no. 3, pp. 1499-1513, March 2014

³W. Roh et al., "Millimeter-wave beamforming as an enabling technology for 5G cellular communications: theoretical feasibility and prototype results," in IEEE Communications Magazine, vol. 52, no. 2, pp. 106-113, February 2014

Problem Statement

Hybrid Precoder Design

- **Coupling** between analog and baseband counterpart → **Nonlinear**
- The analog precoder **rely** on a phase-shifters network, which imposes a constant modulus constraint → **Non-convex**
- **Quantization** of the phase shifters → **Combinatorial**

Problem Statement

Hybrid Precoder Design

- **Coupling** between analog and baseband counterpart → **Nonlinear**
- The analog precoder **rely** on a phase-shifters network, which imposes a constant modulus constraint → **Non-convex**
- **Quantization** of the phase shifters → **Combinatorial**

Traditional Methods

- Based on SVD → **complicated bit-allocation**
- Based on GMD → brings great challenge in addressing **non-convex constraints and exploiting sparsity statistics**
- High computational complexity
- Traditional low-complexity schemes realization cost → Hybrid precoding performance degradation

Problem Statement

Hybrid Precoder Design

- **Coupling** between analog and baseband counterpart → **Nonlinear**
- The analog precoder **rely** on a phase-shifters network, which imposes a constant modulus constraint → **Non-convex**
- **Quantization** of the phase shifters → **Combinatorial**

Traditional Methods

- Based on SVD → **complicated bit-allocation**
- Based on GMD → brings great challenge in addressing **non-convex constraints and exploiting sparsity statistics**
- High computational complexity
- Traditional low-complexity schemes realization cost → Hybrid precoding performance degradation

Aim

- To develop a low-complex energy-efficient solution for the hybrid precoder design problem
- To consider the application of deep learning (DL) to develop optimal hybrid precoder

Problem and Methodology I

Problem Formulation ⁴

- System Model

$$\mathbf{y} = \sqrt{\rho}\mathbf{H}\mathbf{A}\mathbf{D}\mathbf{s} + \mathbf{n} = \sqrt{\rho}\mathbf{H}\mathbf{P}\mathbf{s} + \mathbf{n}$$

- Total achievable rate

$$R = \log_2 \left(\left| \mathbf{I}_K + \frac{\rho}{N\sigma^2} \mathbf{H}\mathbf{P}\mathbf{P}^H \mathbf{H}^H \right| \right)$$

⁴X. Gao, L. Dai, S. Han, I. Chih-Lin, and R. W. Heath, "Energy-efficient hybrid analog and digital precoding for mm-wave mimo systems with large antenna arrays", *IEEE Journal on Selected Areas in Communications*, vol. 34, no. 4, pp. 998–1009, 2016 [4]

Problem and Methodology I

Problem Formulation ⁴

- System Model

$$\mathbf{y} = \sqrt{\rho}\mathbf{H}\mathbf{A}\mathbf{D}\mathbf{s} + \mathbf{n} = \sqrt{\rho}\mathbf{H}\mathbf{P}\mathbf{s} + \mathbf{n}$$

- Total achievable rate

$$R = \log_2 \left(\left| \mathbf{I}_K + \frac{\rho}{N\sigma^2} \mathbf{H}\mathbf{P}\mathbf{P}^H \mathbf{H}^H \right| \right)$$

- Target

- Jointly design **A** and **D** to maximize the achievable rate

⁴X. Gao, L. Dai, S. Han, I. Chih-Lin, and R. W. Heath, "Energy-efficient hybrid analog and digital precoding for mm-wave mimo systems with large antenna arrays", *IEEE Journal on Selected Areas in Communications*, vol. 34, no. 4, pp. 998–1009, 2016 [4]

Problem and Methodology I

Problem Formulation ⁴

■ System Model

$$\mathbf{y} = \sqrt{\rho} \mathbf{H} \mathbf{A} \mathbf{D} \mathbf{s} + \mathbf{n} = \sqrt{\rho} \mathbf{H} \mathbf{P} \mathbf{s} + \mathbf{n}$$

■ Total achievable rate

$$R = \log_2 \left(\left| \mathbf{I}_K + \frac{\rho}{N\sigma^2} \mathbf{H} \mathbf{P} \mathbf{P}^H \mathbf{H}^H \right| \right)$$

■ Target

- Jointly design \mathbf{A} and \mathbf{D} to maximize the achievable rate

■ Three non-convex constraints

- **Structure constraint:** $\mathbf{P} = \mathbf{A} \mathbf{D} = \text{diag}\{\bar{\mathbf{a}}_1, \dots, \bar{\mathbf{a}}_N\} \cdot \text{diag}\{d_1, \dots, d_N\}$
- **Amplitude constraint:** The amplitude of non-zero elements of the analog precoding matrix \mathbf{A} is fixed to $1/\sqrt{M}$
- **Power constraint:** $\|\mathbf{P}\|_F \leq N$

⁴X. Gao, L. Dai, S. Han, I. Chih-Lin, and R. W. Heath, "Energy-efficient hybrid analog and digital precoding for mm-wave mimo systems with large antenna arrays", *IEEE Journal on Selected Areas in Communications*, vol. 34, no. 4, pp. 998–1009, 2016 [4]

SIC-based Hybrid Precoding

- The total rate R can be decomposed as

$$R = \sum_{n=1}^N \log_2 \left(1 + \frac{\rho}{N\sigma^2} \mathbf{p}_n^H \mathbf{H}^H \mathbf{T}_{n-1}^{-1} \mathbf{H} \mathbf{p}_n \right)$$

where \mathbf{p}_n be the N -th column of \mathbf{P} , $\mathbf{T}_n = \mathbf{I}_K + \frac{\rho}{N\sigma^2} \mathbf{H} \mathbf{P}_n \mathbf{P}_n^H \mathbf{H}^H$ and $\mathbf{T}_0 = \mathbf{I}_N$

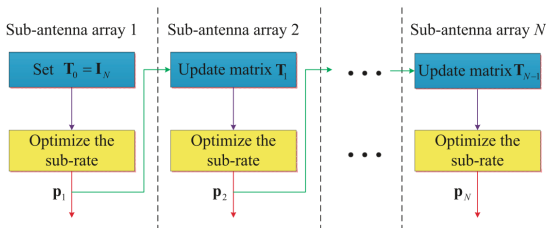
SIC-based Hybrid Precoding

- The total rate R can be decomposed as

$$R = \sum_{n=1}^N \log_2 \left(1 + \frac{\rho}{N\sigma^2} \mathbf{p}_n^H \mathbf{H}^H \mathbf{T}_{n-1}^{-1} \mathbf{H} \mathbf{p}_n \right)$$

where \mathbf{p}_n be the N -th column of \mathbf{P} , $\mathbf{T}_n = \mathbf{I}_K + \frac{\rho}{N\sigma^2} \mathbf{H} \mathbf{P}_n \mathbf{P}_n^H \mathbf{H}^H$ and $\mathbf{T}_0 = \mathbf{I}_N$

- SIC-based hybrid precoding
 - Total rate \rightarrow sub-rate of sub-antenna array
 - Optimize the sub-rate of each sub-antenna array **one by one by** exploiting the concept of SIC for multi-user detection



Solution to the sub-rate optimization problem

- Optimize achievable rate of the n th sub-antenna array

$$\mathbf{p}_n^{\text{opt}} = \arg \max_{\mathbf{p}_n \in \mathcal{F}} \log_2 \left(1 + \frac{\rho}{N\sigma^2} \mathbf{p}_n^H \mathbf{G}_{n-1} \mathbf{p}_n \right)$$

where $\mathbf{G}_{n-1} = \mathbf{H}^H \mathbf{T}_{n-1}^{-1} \mathbf{H}$, \mathcal{F} is the set of all feasible vectors which satisfy all the three constraints

Solution to the sub-rate optimization problem

- Optimize achievable rate of the n th sub-antenna array

$$\mathbf{p}_n^{\text{opt}} = \arg \max_{\mathbf{p}_n \in \mathcal{F}} \log_2 \left(1 + \frac{\rho}{N\sigma^2} \mathbf{p}_n^H \mathbf{G}_{n-1} \mathbf{p}_n \right)$$

where $\mathbf{G}_{n-1} = \mathbf{H}^H \mathbf{T}_{n-1}^{-1} \mathbf{H}$, \mathcal{F} is the set of all feasible vectors which satisfy all the three constraints

- Considering non-zero elements, it is equivalent to a simplified problem as

$$\bar{\mathbf{p}}_n^{\text{opt}} = \arg \max_{\bar{\mathbf{p}}_n \in \bar{\mathcal{F}}} \log_2 \left(1 + \frac{\rho}{N\sigma^2} \bar{\mathbf{p}}_n^H \bar{\mathbf{G}}_{n-1} \bar{\mathbf{p}}_n \right)$$

where $\bar{\mathbf{G}}_{n-1} = \mathbf{R} \mathbf{G}_{n-1} \mathbf{R}^H$, $\mathbf{R} = [\mathbf{0}_{M \times M(n-1)} \quad \mathbf{I}_M \quad \mathbf{0}_{M \times M(N-n)}]$ is the corresponding selection matrix

Solution to the sub-rate optimization problem

- Optimize achievable rate of the n th sub-antenna array

$$\mathbf{p}_n^{\text{opt}} = \arg \max_{\mathbf{p}_n \in \mathcal{F}} \log_2 \left(1 + \frac{\rho}{N\sigma^2} \mathbf{p}_n^H \mathbf{G}_{n-1} \mathbf{p}_n \right)$$

where $\mathbf{G}_{n-1} = \mathbf{H}^H \mathbf{T}_{n-1}^{-1} \mathbf{H}$, \mathcal{F} is the set of all feasible vectors which satisfy all the three constraints

- Considering non-zero elements, it is equivalent to a simplified problem as

$$\bar{\mathbf{p}}_n^{\text{opt}} = \arg \max_{\bar{\mathbf{p}}_n \in \tilde{\mathcal{F}}} \log_2 \left(1 + \frac{\rho}{N\sigma^2} \bar{\mathbf{p}}_n^H \tilde{\mathbf{G}}_{n-1} \bar{\mathbf{p}}_n \right)$$

where $\tilde{\mathbf{G}}_{n-1} = \mathbf{R} \mathbf{G}_{n-1} \mathbf{R}^H$, $\mathbf{R} = [\mathbf{0}_{M \times M(n-1)} \quad \mathbf{I}_M \quad \mathbf{0}_{M \times M(N-n)}]$ is the corresponding selection matrix

- Simplify the optimization problem $\bar{\mathbf{p}}_n^{\text{opt}} = \arg \min_{\bar{\mathbf{p}}_n \in \tilde{\mathcal{F}}} \|\mathbf{v}_1 - \bar{\mathbf{p}}_n\|_2^2$, where \mathbf{v}_1 is the first right singular vector of $\tilde{\mathbf{G}}_{n-1}$

Solution to the sub-rate optimization problem

- Optimize achievable rate of the n th sub-antenna array

$$\mathbf{p}_n^{\text{opt}} = \arg \max_{\mathbf{p}_n \in \mathcal{F}} \log_2 \left(1 + \frac{\rho}{N\sigma^2} \mathbf{p}_n^H \mathbf{G}_{n-1} \mathbf{p}_n \right)$$

where $\mathbf{G}_{n-1} = \mathbf{H}^H \mathbf{T}_{n-1}^{-1} \mathbf{H}$, \mathcal{F} is the set of all feasible vectors which satisfy all the three constraints

- Considering non-zero elements, it is equivalent to a simplified problem as

$$\bar{\mathbf{p}}_n^{\text{opt}} = \arg \max_{\bar{\mathbf{p}}_n \in \tilde{\mathcal{F}}} \log_2 \left(1 + \frac{\rho}{N\sigma^2} \bar{\mathbf{p}}_n^H \tilde{\mathbf{G}}_{n-1} \bar{\mathbf{p}}_n \right)$$

where $\tilde{\mathbf{G}}_{n-1} = \mathbf{R} \mathbf{G}_{n-1} \mathbf{R}^H$, $\mathbf{R} = [\mathbf{0}_{M \times M(n-1)} \quad \mathbf{I}_M \quad \mathbf{0}_{M \times M(N-n)}]$ is the corresponding selection matrix

- Simplify the optimization problem $\bar{\mathbf{p}}_n^{\text{opt}} = \arg \min_{\bar{\mathbf{p}}_n \in \tilde{\mathcal{F}}} \|\mathbf{v}_1 - \bar{\mathbf{p}}_n\|_2^2$, where \mathbf{v}_1 is the first right singular vector of $\tilde{\mathbf{G}}_{n-1}$
- Find a feasible precoding vector $\bar{\mathbf{p}}_n$, sufficiently close to \mathbf{v}_1 , to maximize the achievable sub-rate

Design of Analog and Digital Precoder

■ Problem

- As we have $\bar{\mathbf{p}}_n = d_n \bar{\mathbf{a}}_n$, $\|\mathbf{v}_1 - \bar{\mathbf{p}}_n\|_2^2$ equals to

$$\|\mathbf{v}_1 - \bar{\mathbf{p}}_n\|_2^2 = (d_n - \text{Re}(\mathbf{v}_1^H \bar{\mathbf{a}}_n))^2 + (1 - [\text{Re}(\mathbf{v}_1^H \bar{\mathbf{a}}_n)]^2)$$

Design of Analog and Digital Precoder

■ Problem

- As we have $\bar{\mathbf{p}}_n = d_n \bar{\mathbf{a}}_n$, $\|\mathbf{v}_1 - \bar{\mathbf{p}}_n\|_2^2$ equals to

$$\|\mathbf{v}_1 - \bar{\mathbf{p}}_n\|_2^2 = (d_n - \text{Re}(\mathbf{v}_1^H \bar{\mathbf{a}}_n))^2 + (1 - [\text{Re}(\mathbf{v}_1^H \bar{\mathbf{a}}_n)]^2)$$

■ Solution

- Analog precoder: $\bar{\mathbf{a}}_n^{\text{opt}} = \frac{1}{\sqrt{M}} e^{j\text{angle}(\mathbf{v}_1)}$
- Digital precoder: $d_n^{\text{opt}} = \text{Re}(\mathbf{v}_1^H \bar{\mathbf{a}}_n) = \frac{1}{\sqrt{M}} \text{Re}(\mathbf{v}_1^H e^{j\text{angle}(\mathbf{v}_1)}) = \frac{\|\mathbf{v}_1\|_1}{\sqrt{M}}$
- Hybrid precoder: $\bar{\mathbf{p}}_n^{\text{opt}} = \frac{1}{M} \|\mathbf{v}_1\|_1 e^{j\text{angle}(\mathbf{v}_1)}$
- All the **three constraints** are **satisfied**

Design of Analog and Digital Precoder

■ Problem

- As we have $\bar{\mathbf{p}}_n = d_n \bar{\mathbf{a}}_n$, $\|\mathbf{v}_1 - \bar{\mathbf{p}}_n\|_2^2$ equals to

$$\|\mathbf{v}_1 - \bar{\mathbf{p}}_n\|_2^2 = (d_n - \text{Re}(\mathbf{v}_1^H \bar{\mathbf{a}}_n))^2 + (1 - [\text{Re}(\mathbf{v}_1^H \bar{\mathbf{a}}_n)]^2)$$

■ Solution

- Analog precoder: $\bar{\mathbf{a}}_n^{\text{opt}} = \frac{1}{\sqrt{M}} e^{j\text{angle}(\mathbf{v}_1)}$
- Digital precoder: $d_n^{\text{opt}} = \text{Re}(\mathbf{v}_1^H \bar{\mathbf{a}}_n) = \frac{1}{\sqrt{M}} \text{Re}(\mathbf{v}_1^H e^{j\text{angle}(\mathbf{v}_1)}) = \frac{\|\mathbf{v}_1\|_1}{\sqrt{M}}$
- Hybrid precoder: $\bar{\mathbf{p}}_n^{\text{opt}} = \frac{1}{M} \|\mathbf{v}_1\|_1 e^{j\text{angle}(\mathbf{v}_1)}$
- All the three constraints are satisfied

■ Summary

- SVD of $\tilde{\mathbf{G}}_{n-1}$ to obtain \mathbf{v}_1
- Compute $\bar{\mathbf{p}}_n^{\text{opt}} = \frac{1}{M} \|\mathbf{v}_1\|_1 e^{j\text{angle}(\mathbf{v}_1)}$ for the n -th sub-antenna array
- Update $\tilde{\mathbf{G}}_n$ for the $(n+1)$ -th sub-antenna array

Low-Complexity Solution

■ Computation of \mathbf{v}_1

- Only the first right singular vector of $\tilde{\mathbf{G}}_{n-1}$ is required
- Realized by power iteration algorithm with complexity $O(M^2)$

⁵O. E. Ayach, S. Rajagopal, S. Abu-Surra, Z. Pi and R. W. Heath, "Spatially Sparse Precoding in Millimeter Wave MIMO Systems," in IEEE Transactions on Wireless Communications, vol. 13, no. 3, pp. 1499-1513, March 2014 [2]

Low-Complexity Solution

- Computation of \mathbf{v}_1
 - Only the first right singular vector of $\tilde{\mathbf{G}}_{n-1}$ is required
 - Realized by power iteration algorithm with complexity $O(M^2)$
- Acquire the optimal hybrid precoder
 - The complexity is only $O(M^2)$ to obtain $\tilde{\mathbf{p}}_n^{\text{opt}} = \frac{1}{M} \|\mathbf{v}_1\|_1 e^{j\angle(\mathbf{v}_1)}$

⁵O. E. Ayach, S. Rajagopal, S. Abu-Surra, Z. Pi and R. W. Heath, "Spatially Sparse Precoding in Millimeter Wave MIMO Systems," in IEEE Transactions on Wireless Communications, vol. 13, no. 3, pp. 1499-1513, March 2014 [2]

Low-Complexity Solution

- Computation of \mathbf{v}_1
 - Only the first right singular vector of $\tilde{\mathbf{G}}_{n-1}$ is required
 - Realized by power iteration algorithm with complexity $O(M^2)$
- Acquire the optimal hybrid precoder
 - The complexity is only $O(M^2)$ to obtain $\tilde{\mathbf{p}}_n^{\text{opt}} = \frac{1}{M} \|\mathbf{v}_1\|_1 e^{j\angle(\mathbf{v}_1)}$
- Update $\tilde{\mathbf{G}}_n$
 - The calculation can be simplified as

$$\tilde{\mathbf{G}}_n \approx \tilde{\mathbf{G}}_{n-1} - \frac{\frac{\rho}{N\sigma^2} \Sigma_1^2 \mathbf{v}_1 \mathbf{v}_1^H}{1 + \frac{\rho}{N\sigma^2} \Sigma_1}$$

where Σ_1 is the largest singular value of $\tilde{\mathbf{G}}_{n-1}$

- Corresponding complexity is $O(M^2)$

⁵O. E. Ayach, S. Rajagopal, S. Abu-Surra, Z. Pi and R. W. Heath, "Spatially Sparse Precoding in Millimeter Wave MIMO Systems," in IEEE Transactions on Wireless Communications, vol. 13, no. 3, pp. 1499-1513, March 2014 [2]

Low-Complexity Solution

- Computation of \mathbf{v}_1
 - Only the first right singular vector of $\tilde{\mathbf{G}}_{n-1}$ is required
 - Realized by power iteration algorithm with complexity $O(M^2)$
- Acquire the optimal hybrid precoder
 - The complexity is only $O(M^2)$ to obtain $\tilde{\mathbf{p}}_n^{\text{opt}} = \frac{1}{M} \|\mathbf{v}_1\|_1 e^{j\angle(\mathbf{v}_1)}$
- Update $\tilde{\mathbf{G}}_n$
 - The calculation can be simplified as

$$\tilde{\mathbf{G}}_n \approx \tilde{\mathbf{G}}_{n-1} - \frac{\frac{\rho}{N\sigma^2} \Sigma_1^2 \mathbf{v}_1 \mathbf{v}_1^H}{1 + \frac{\rho}{N\sigma^2} \Sigma_1}$$

where Σ_1 is the largest singular value of $\tilde{\mathbf{G}}_{n-1}$

- Corresponding complexity is $O(M^2)$
- Total complexity $O(M^2(NS + K))$
 - Only 10% of SVD-based spatially sparse precoding⁵

⁵O. E. Ayach, S. Rajagopal, S. Abu-Surra, Z. Pi and R. W. Heath, "Spatially Sparse Precoding in Millimeter Wave MIMO Systems," in IEEE Transactions on Wireless Communications, vol. 13, no. 3, pp. 1499-1513, March 2014 [2]

Achievable Rate

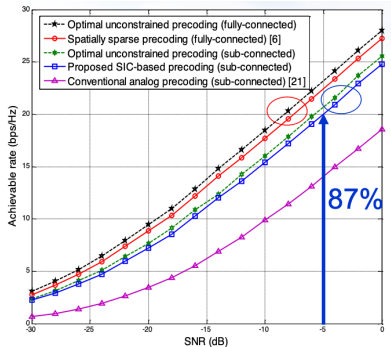
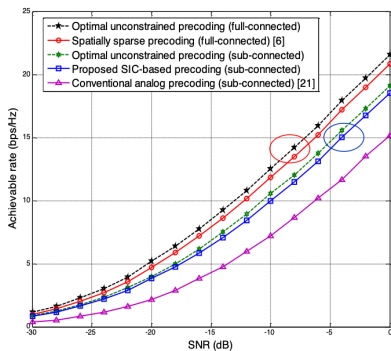
■ Simulation Setup

- Antenna: (1) $NM \times K = 64 \times 16$ (2) $NM \times K = 128 \times 32$
- RF chains: (1) $N = 8$ (2) $N = 16$
- Channel: Geometric Saleh-Valenzuela model

Achievable Rate

■ Simulation Setup

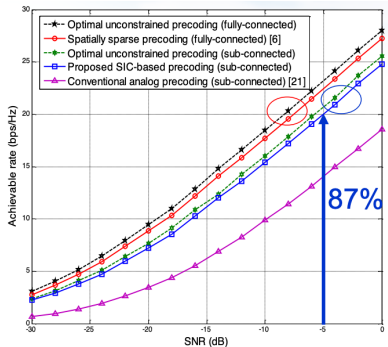
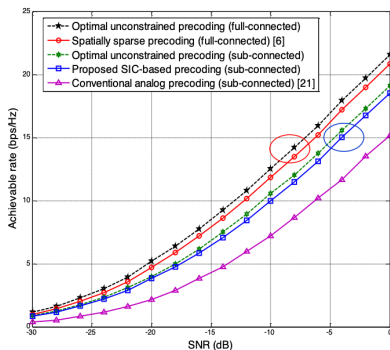
- Antenna: (1) $NM \times K = 64 \times 16$ (2) $NM \times K = 128 \times 32$
- RF chains: (1) $N = 8$ (2) $N = 16$
- Channel: Geometric Saleh-Valenzuela model



Achievable Rate

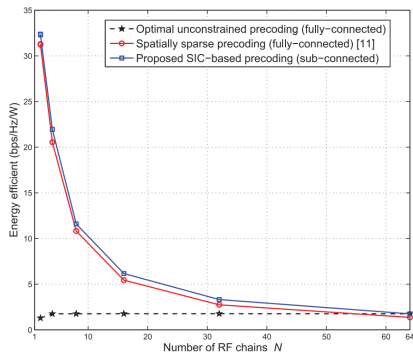
■ Simulation Setup

- Antenna: (1) $NM \times K = 64 \times 16$ (2) $NM \times K = 128 \times 32$
- RF chains: (1) $N = 8$ (2) $N = 16$
- Channel: Geometric Saleh-Valenzuela model



SIC-based hybrid precoding is near-optimal!

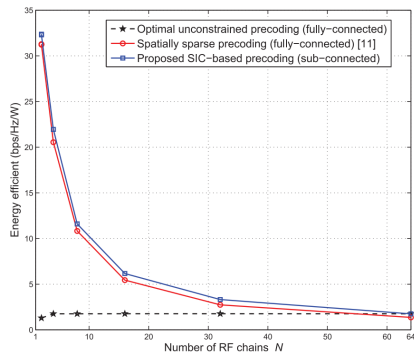
Energy Efficiency



- Both the SIC-based precoding and the spatially sparse precoding⁶ can achieve higher **energy-efficiency** than the optimal unconstrained precoding.

⁶O. E. Ayach, S. Rajagopal, S. Abu-Surra, Z. Pi and R. W. Heath, "Spatially Sparse Precoding in Millimeter Wave MIMO Systems," in IEEE Transactions on Wireless Communications, vol. 13, no. 3, pp. 1499-1513, March 2014 [2]

Energy Efficiency



- Both the SIC-based precoding and the spatially sparse precoding⁶ can achieve higher **energy-efficiency** than the optimal unconstrained precoding.

SIC-based hybrid precoding is more energy-efficient!

⁶O. E. Ayach, S. Rajagopal, S. Abu-Surra, Z. Pi and R. W. Heath, "Spatially Sparse Precoding in Millimeter Wave MIMO Systems," in IEEE Transactions on Wireless Communications, vol. 13, no. 3, pp. 1499-1513, March 2014 [2]

Problem and Methodology II

Problem Formulation ⁷

- System Model

$$\mathbf{x} = \mathbf{D}\mathbf{s}$$

$$\mathbf{y} = \mathbf{B}^H \mathbf{H} \mathbf{x} + \mathbf{B}^H \mathbf{n}$$

- Here, $\mathbf{D} = \mathbf{D}_A \mathbf{D}_D$ and $\mathbf{B} = \mathbf{B}_A \mathbf{B}_D$

⁷H. Huang, Y. Song, J. Yang, G. Gui, and F. Adachi, "Deep-learning-based millimeter-wave massive mimo for hybrid precoding", *IEEE Transactions on Vehicular Technology*, vol. 68, no. 3, pp. 3027–3032, 2019 [5]

Problem and Methodology II

Problem Formulation ⁷

- System Model

$$\mathbf{x} = \mathbf{D}\mathbf{s}$$

$$\mathbf{y} = \mathbf{B}^H \mathbf{H} \mathbf{x} + \mathbf{B}^H \mathbf{n}$$

- Here, $\mathbf{D} = \mathbf{D}_A \mathbf{D}_D$ and $\mathbf{B} = \mathbf{B}_A \mathbf{B}_D$

- Transmit power constraint:

$$\text{tr}\{\mathbf{D}\mathbf{D}^H\} \leq N_s$$

⁷H. Huang, Y. Song, J. Yang, G. Gui, and F. Adachi, "Deep-learning-based millimeter-wave massive mimo for hybrid precoding", *IEEE Transactions on Vehicular Technology*, vol. 68, no. 3, pp. 3027–3032, 2019 [5]

Problem and Methodology II

Problem Formulation ⁷

- System Model

$$\mathbf{x} = \mathbf{D}\mathbf{s}$$

$$\mathbf{y} = \mathbf{B}^H \mathbf{H} \mathbf{x} + \mathbf{B}^H \mathbf{n}$$

- Here, $\mathbf{D} = \mathbf{D}_A \mathbf{D}_D$ and $\mathbf{B} = \mathbf{B}_A \mathbf{B}_D$

- Transmit power constraint:

$$\text{tr}\{\mathbf{D}\mathbf{D}^H\} \leq N_s$$

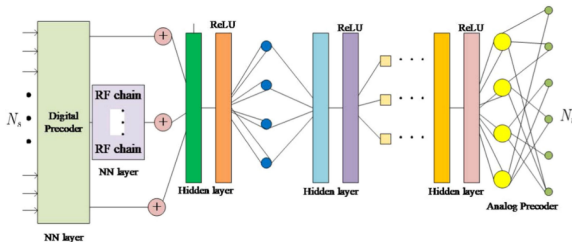
- Constraints on the elements of \mathbf{D}_A and \mathbf{B}_A :

$$|\{\mathbf{D}_A\}_{i,j}| = \frac{1}{\sqrt{N_t}}, \quad |\{\mathbf{B}_A\}_{i,j}| = \frac{1}{\sqrt{N_r}}$$

⁷H. Huang, Y. Song, J. Yang, G. Gui, and F. Adachi, "Deep-learning-based millimeter-wave massive mimo for hybrid precoding", *IEEE Transactions on Vehicular Technology*, vol. 68, no. 3, pp. 3027–3032, 2019 [5]

Deep-Neural Network

DNN Framework



- Input Layer: 128 units
- Hidden Layers: 400 units and 256 units
- Noise Layer: 200 units
- Hidden Layers: 128 units and 64 units
- Output Layer: Deployed to generate output signals
- Input and hidden layers activation: ReLU
- Output layer activation:

$$f(s) = \min(\max(s, 0), N_s)$$

Learning Policy

- Decompose \mathbf{H} using GMD as

$$\mathbf{H} = \mathbf{W}\mathbf{Q}\mathbf{R}^H = [\mathbf{W}_1, \mathbf{W}_2] \begin{bmatrix} \mathbf{Q}_1 & * \\ \mathbf{0} & \mathbf{Q}_2 \end{bmatrix} \begin{bmatrix} \mathbf{R}_1^H \\ \mathbf{R}_2^H \end{bmatrix}$$

- The largest N_s singular values: $q_{i,i} = (\delta_1, \delta_2, \dots, \delta_{N_s})^{\frac{1}{N_s}} \in \bar{\mathbf{q}} \ \forall i$

Learning Policy

- Decompose \mathbf{H} using GMD as

$$\mathbf{H} = \mathbf{W}\mathbf{Q}\mathbf{R}^H = [\mathbf{W}_1, \mathbf{W}_2] \begin{bmatrix} \mathbf{Q}_1 & * \\ \mathbf{0} & \mathbf{Q}_2 \end{bmatrix} \begin{bmatrix} \mathbf{R}_1^H \\ \mathbf{R}_2^H \end{bmatrix}$$

- The largest N_s singular values: $q_{i,i} = (\delta_1, \delta_2, \dots, \delta_{N_s})^{\frac{1}{N_s}} \in \bar{\mathbf{q}} \forall i$
- The received signal is given as

$$\begin{aligned} \mathbf{y} &= \mathbf{W}_1^H \mathbf{H} \mathbf{R}_1 \mathbf{s} + \mathbf{W}_1^H \mathbf{n} \\ &= \mathbf{Q}_1 \mathbf{s} + \mathbf{W}_1^H \mathbf{n} \end{aligned}$$

Learning Policy

- Decompose \mathbf{H} using GMD as

$$\mathbf{H} = \mathbf{W}\mathbf{Q}\mathbf{R}^H = [\mathbf{W}_1, \mathbf{W}_2] \begin{bmatrix} \mathbf{Q}_1 & * \\ \mathbf{0} & \mathbf{Q}_2 \end{bmatrix} \begin{bmatrix} \mathbf{R}_1^H \\ \mathbf{R}_2^H \end{bmatrix}$$

- The largest N_s singular values: $q_{i,i} = (\delta_1, \delta_2, \dots, \delta_{N_s})^{\frac{1}{N_s}} \in \bar{\mathbf{q}} \forall i$
- The received signal is given as

$$\begin{aligned} \mathbf{y} &= \mathbf{W}_1^H \mathbf{H} \mathbf{R}_1 \mathbf{s} + \mathbf{W}_1^H \mathbf{n} \\ &= \mathbf{Q}_1 \mathbf{s} + \mathbf{W}_1^H \mathbf{n} \end{aligned}$$

- The **loss** function is given as

$$loss = \|\mathbf{R}_1 - \mathbf{R}_A \mathbf{R}_D\|_F = \sqrt{\sum_{i=1}^{\min\{N_t, N_s\}} \delta_i^2 (\mathbf{R}_1 - \mathbf{R}_A \mathbf{R}_D)}$$

where \mathbf{R}_A and \mathbf{R}_D are the GMD-based analog and digital precoder, respectively and $\delta_i(\mathbf{R}_1 - \mathbf{R}_A \mathbf{R}_D)$ implies the singular values of matrix $(\mathbf{R}_1 - \mathbf{R}_A \mathbf{R}_D)$

Learning Policy

- Decompose \mathbf{H} using GMD as

$$\mathbf{H} = \mathbf{W}\mathbf{Q}\mathbf{R}^H = [\mathbf{W}_1, \mathbf{W}_2] \begin{bmatrix} \mathbf{Q}_1 & * \\ \mathbf{0} & \mathbf{Q}_2 \end{bmatrix} \begin{bmatrix} \mathbf{R}_1^H \\ \mathbf{R}_2^H \end{bmatrix}$$

- The largest N_s singular values: $q_{i,i} = (\delta_1, \delta_2, \dots, \delta_{N_s})^{\frac{1}{N_s}} \in \bar{\mathbf{q}} \forall i$
- The received signal is given as

$$\begin{aligned} \mathbf{y} &= \mathbf{W}_1^H \mathbf{H} \mathbf{R}_1 \mathbf{s} + \mathbf{W}_1^H \mathbf{n} \\ &= \mathbf{Q}_1 \mathbf{s} + \mathbf{W}_1^H \mathbf{n} \end{aligned}$$

- The **loss** function is given as

$$loss = \|\mathbf{R}_1 - \mathbf{R}_A \mathbf{R}_D\|_F = \sqrt{\sum_{i=1}^{\min\{N_t, N_s\}} \delta_i^2} (\mathbf{R}_1 - \mathbf{R}_A \mathbf{R}_D)$$

where \mathbf{R}_A and \mathbf{R}_D are the GMD-based analog and digital precoder, respectively and $\delta_i(\mathbf{R}_1 - \mathbf{R}_A \mathbf{R}_D)$ implies the singular values of matrix $(\mathbf{R}_1 - \mathbf{R}_A \mathbf{R}_D)$

- These constraints need to be satisfied:

$$|\{\mathbf{R}_A\}_{i,j}| = \frac{1}{\sqrt{N_t}}, \quad \text{tr}(\mathbf{R}_A \mathbf{R}_D \mathbf{R}_D^H \mathbf{R}_A^H) \leq N_s$$

Autoencoder

- To construct an autoencoder, the deep-neural network (DNN) framework is employed as

$$\mathbf{R}_1 = f(\mathbf{R}_A \mathbf{R}_D; \Omega)$$

where Ω is the dataset of the samples and $f(\cdot)$ is the mapping relation.

Autoencoder

- To construct an autoencoder, the deep-neural network (DNN) framework is employed as

$$\mathbf{R}_1 = f(\mathbf{R}_A \mathbf{R}_D; \Omega)$$

where Ω is the dataset of the samples and $f(\cdot)$ is the mapping relation.

- **Training Procedure:**

- $\mathbf{R}_A, \mathbf{R}_D$ - Empty matrices
 - The DNN is trained with the input data sequences
 - Update $\mathbf{R}_A, \mathbf{R}_D$
 - AoA θ_p^r , AoD θ_p^t - generated randomly
 - Bias between \mathbf{R}_1 and $\mathbf{R}_A \mathbf{R}_D$ - from the output layer
- The training set Ω is obtained

Stochastic Gradient Descent

- SGD algorithm with momentum to process the loss function

$$\mathbf{R}_A^{j+1} = \mathbf{R}_A^j + v \quad (1)$$

$$\mathbf{R}_D^{j+1} = \mathbf{R}_D^j + v \quad (2)$$

where v is the velocity for facilitating the gradient element and j represents the iteration

Stochastic Gradient Descent

- SGD algorithm with momentum to process the loss function

$$\mathbf{R}_A^{j+1} = \mathbf{R}_A^j + v \quad (1)$$

$$\mathbf{R}_D^{j+1} = \mathbf{R}_D^j + v \quad (2)$$

where v is the velocity for facilitating the gradient element and j represents the iteration

- The update procedure of v can be given as

$$\begin{aligned} v &= \alpha v - \varepsilon g \\ &= \alpha v - \varepsilon \frac{1}{N} \nabla_{\mathbf{R}_A, \mathbf{R}_D} \sqrt{\sum_{i=1}^{\min\{N_t, N_s\}} \delta_i^2 (\mathbf{R}_1 - \mathbf{R}_A \mathbf{R}_D)}, \end{aligned} \quad (3)$$

where α is the momentum parameter and ε is the learning rate. Also, g and N are the gradient element and the number of samples, respectively

Stochastic Gradient Descent

- SGD algorithm with momentum to process the loss function

$$\mathbf{R}_A^{j+1} = \mathbf{R}_A^j + v \quad (1)$$

$$\mathbf{R}_D^{j+1} = \mathbf{R}_D^j + v \quad (2)$$

where v is the velocity for facilitating the gradient element and j represents the iteration

- The update procedure of v can be given as

$$\begin{aligned} v &= \alpha v - \varepsilon g \\ &= \alpha v - \varepsilon \frac{1}{N} \nabla_{\mathbf{R}_A, \mathbf{R}_D} \sqrt{\sum_{i=1}^{\min\{N_t, N_s\}} \delta_i^2 (\mathbf{R}_1 - \mathbf{R}_A \mathbf{R}_D)}, \end{aligned} \quad (3)$$

where α is the momentum parameter and ε is the learning rate. Also, g and N are the gradient element and the number of samples, respectively

- DL-based scheme has the **lowest complexity**, where the number of multiplications and divisions are $O(N_s N_t^2)$ and $O(L^2)$, respectively

Numerical Results

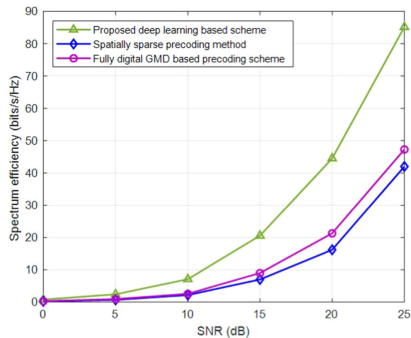
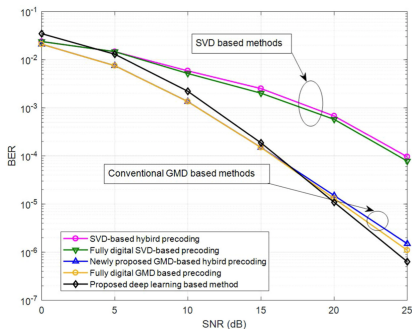
■ Simulation Setup

- Channel: Geometric Saleh-Valenzuela (SV) model with $P=3$ at 28 GHz
- Angles are generated randomly in $\{-\pi/2, \pi/2\}$
- To generate channel measurements: Environment simulator
- To construct and process the DNN framework: *Keras*
- Learning rate 0.001, momentum of 0.85

Numerical Results

■ Simulation Setup

- Channel: Geometric Saleh-Valenzuela (SV) model with $P=3$ at 28 GHz
- Angles are generated randomly in $\{-\pi/2, \pi/2\}$
- To generate channel measurements: Environment simulator
- To construct and process the DNN framework: *Keras*
- Learning rate 0.001, momentum of 0.85



DL-based scheme is superior!

Critical Review and Future Work

- **Critical Points**

- Single user scenario

Critical Review and Future Work

■ Critical Points

- Single user scenario
- Infinite or high-resolution phase shifters (PSs)

Critical Review and Future Work

■ Critical Points

- Single user scenario
- Infinite or high-resolution phase shifters (PSs)
- The number of RF chains with high-resolution DACs/ADCs

Critical Review and Future Work

■ Critical Points

- Single user scenario
- Infinite or high-resolution phase shifters (PSs)
- The number of RF chains with high-resolution DACs/ADCs
- The channel model as a narrowband mm-Wave channel

Critical Review and Future Work

■ Critical Points

- Single user scenario
- Infinite or high-resolution phase shifters (PSs)
- The number of RF chains with high-resolution DACs/ADCs
- The channel model as a narrowband mm-Wave channel
- Further, SGD with momentum is good for computation in less time, but not reliable

Critical Review and Future Work

■ Critical Points

- Single user scenario
- Infinite or high-resolution phase shifters (PSs)
- The number of RF chains with high-resolution DACs/ADCs
- The channel model as a narrowband mm-Wave channel
- Further, SGD with momentum is good for computation in less time, but not reliable

■ Future Work

- Design of optimal hybrid precoders for multi-user systems
- To address the high energy consumption problem, the usage of low-resolution PSs [6, 7] and low-resolution DACs/ADCs [8, 9, 10]

Critical Review and Future Work

■ Critical Points

- Single user scenario
- Infinite or high-resolution phase shifters (PSs)
- The number of RF chains with high-resolution DACs/ADCs
- The channel model as a narrowband mm-Wave channel
- Further, SGD with momentum is good for computation in less time, but not reliable

■ Future Work

- Design of optimal hybrid precoders for multi-user systems
- To address the high energy consumption problem, the usage of low-resolution PSs [6, 7] and low-resolution DACs/ADCs [8, 9, 10]
- An appropriate trade-off between energy efficiency and system sum-rate for a wideband mm-Wave channel is still an open research problem

Critical Review and Future Work

■ Critical Points

- Single user scenario
- Infinite or high-resolution phase shifters (PSs)
- The number of RF chains with high-resolution DACs/ADCs
- The channel model as a narrowband mm-Wave channel
- Further, SGD with momentum is good for computation in less time, but not reliable

■ Future Work

- Design of optimal hybrid precoders for multi-user systems
- To address the high energy consumption problem, the usage of low-resolution PSs [6, 7] and low-resolution DACs/ADCs [8, 9, 10]
- An appropriate trade-off between energy efficiency and system sum-rate for a wideband mm-Wave channel is still an open research problem
- To solve the design of finding the best hybrid precoder the idea of cross-entropy optimization (CEO) in deep learning solutions [11]

Critical Review and Future Work

■ Critical Points

- Single user scenario
- Infinite or high-resolution phase shifters (PSs)
- The number of RF chains with high-resolution DACs/ADCs
- The channel model as a narrowband mm-Wave channel
- Further, SGD with momentum is good for computation in less time, but not reliable

■ Future Work

- Design of optimal hybrid precoders for multi-user systems
- To address the high energy consumption problem, the usage of low-resolution PSs [6, 7] and low-resolution DACs/ADCs [8, 9, 10]
- An appropriate trade-off between energy efficiency and system sum-rate for a wideband mm-Wave channel is still an open research problem
- To solve the design of finding the best hybrid precoder the idea of cross-entropy optimization (CEO) in deep learning solutions [11]

It could be more practical and of great benefit to leverage deep learning (DL) in mm-Wave massive MIMO systems!

References I



P. V. Amadori and C. Masouros, “Low rf-complexity millimeter-wave beamspace-mimo systems by beam selection,” *IEEE Transactions on Communications*, vol. 63, no. 6, pp. 2212–2223, 2015.



O. El Ayach, S. Rajagopal, S. Abu-Surra, Z. Pi, and R. W. Heath, “Spatially sparse precoding in millimeter wave mimo systems,” *IEEE transactions on wireless communications*, vol. 13, no. 3, pp. 1499–1513, 2014.



W. Roh, J.-Y. Seol, J. Park, B. Lee, J. Lee, Y. Kim, J. Cho, K. Cheun, and F. Aryanfar, “Millimeter-wave beamforming as an enabling technology for 5g cellular communications: Theoretical feasibility and prototype results,” *IEEE communications magazine*, vol. 52, no. 2, pp. 106–113, 2014.



X. Gao, L. Dai, S. Han, I. Chih-Lin, and R. W. Heath, “Energy-efficient hybrid analog and digital precoding for mmwave mimo systems with large antenna arrays,” *IEEE Journal on Selected Areas in Communications*, vol. 34, no. 4, pp. 998–1009, 2016.



H. Huang, Y. Song, J. Yang, G. Gui, and F. Adachi, “Deep-learning-based millimeter-wave massive mimo for hybrid precoding,” *IEEE Transactions on Vehicular Technology*, vol. 68, no. 3, pp. 3027–3032, 2019.



X. Gao, L. Dai, Y. Sun, S. Han, and I. Chih-Lin, “Machine learning inspired energy-efficient hybrid precoding for mmwave massive mimo systems,” *2017 IEEE International Conference on Communications (ICC)*, pp. 1–6, 2017.

References II



S. Gao, Y. Dong, C. Chen, and Y. Jin, “Hierarchical beam selection in mmwave multiuser mimo systems with one-bit analog phase shifters,” *2016 8th International Conference on Wireless Communications & Signal Processing (WCSP)*, pp. 1–5, 2016.



Y. Dong and L. Qiu, “Spectral efficiency of massive mimo systems with low-resolution adcs and mmse receiver,” *IEEE Communications Letters*, vol. 21, no. 8, pp. 1771–1774, 2017.



J. Zhang, L. Dai, S. Sun, and Z. Wang, “On the spectral efficiency of massive mimo systems with low-resolution adcs,” *IEEE Communications Letters*, vol. 20, no. 5, pp. 842–845, 2016.



C. Kong, C. Zhong, S. Jin, S. Yang, H. Lin, and Z. Zhang, “Full-duplex massive mimo relaying systems with low-resolution adcs,” *IEEE Transactions on Wireless Communications*, vol. 16, no. 8, pp. 5033–5047, 2017.



R. Y. Rubinstein and D. P. Kroese, “Simulation and the monte carlo method,” *John Wiley & Sons*, vol. 10, 2016.

Thank You